

# Comparable Electron Capture Efficiencies for Various Protonated Sites on the 3<sup>rd</sup> Generation Poly(Propylene Imine) Dendrimer Ions: Applications by SORI-CAD and Electron Capture Dissociation Mass Spectrometry (ECD MS)

Sang Yun Han,<sup>†,a</sup> Sunyoung Lee,<sup>a</sup> and Han Bin Oh<sup>\*</sup>

Department of Chemistry and Interdisciplinary Program of Integrated Biotechnology, Sogang University, Seoul 121-742, Korea

<sup>\*</sup>E-mail: hanbinoh@sogang.ac.kr

<sup>†</sup>Division of Chemical Metrology and Material Evaluation, Korea Research Institute of Standards and Science, Daejeon 305-340, Korea

Received March 1, 2005

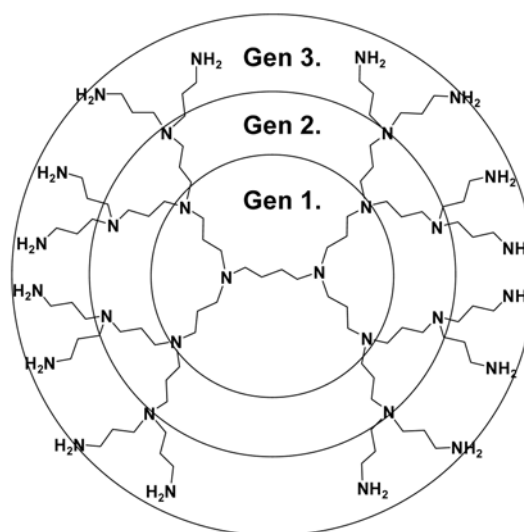
In this article, we report the tandem mass spectrometry investigations for the electron capture efficiencies of the protons belonging to the different locations (generations) in a poly(propylene imine) dendrimer with three layers of a repeat unit (named as the third generation dendrimer). The employed tandem mass spectrometry methods include SORI-CAD (sustained off-resonance irradiation collisional activation dissociation) and ECD (electron capture dissociation) mass spectrometry. We obtained SORI-CAD spectra for the dendrimer ions in the different charge states, ranging from 2+ to 4+. The analysis of fragmentation sites provides the information as to where the protons are distributed among various generations of the dendrimer. Based upon this, a new strategy to study the electron capture efficiencies of the protons is utilized to examine a new type of triply-charged ions by SORI-CAD, *i.e.*, the 3+ ions generated from the charge reduction of the native 4+ ions by ECD:  $(M+4H)^{4+} + e^- \rightarrow (M+4H)^{3+\bullet} \rightarrow (H^{\bullet}_{\text{ejected}}) + (M+3H)^{3+} \rightarrow \text{CAD}$ . Interestingly, comparison of these four SORI-CAD spectra indicates that the proton distribution in the charge-reduced 3+ ions is very close to that in the native 4+ ions. It further suggests that in this synthetic polymer (~1.7 kDa) with an artificial architecture, the electron capture efficiencies of the protons are actually insensitive to where they are located in the molecule. This is somewhat contradictory to common expectations that the protons in the inner generations may not be well exposed to the incoming electron irradiation as much as the outer ones are, thus may be less efficient for electron capture. This finding may carry some implications for the case of medium sized peptide ions with similar masses, which are known to show no obvious site-specific fragmentations in ECD MS.

**Key Words :** Poly(propylene imine) dendrimer, Fourier transform mass spectrometry (FTMS), Electron capture dissociation, Sustained off-resonance irradiation collision activation dissociation (SORI-CAD), Proton distribution

## Introduction

In recent years, dendritic polymers have been a subject of tremendous interest due to its unique structure and potential as a drug deliverer.<sup>1-3</sup> Its diversity in size, chemical property, and symmetry of the branching unit has required sophisticated tools for the structural analysis.<sup>4</sup> In this respect, mass spectrometry has been successful since the advent of soft ionization mass spectrometry methods such as electrospray ionization (ESI) and matrix assisted laser desorption/ionization (MALDI).<sup>5,6</sup>

Of many hyperbranched dendritic polymers, poly(propylene imine) dendrimer has been most intensively studied, utilizing a variety of mass spectrometry analyzers.<sup>7-9</sup> This dendritic polymer contains a 1,4-diaminobutane (DAB) core that is connected to tertiary nitrogens through propylenes and also multiple layers of a repeat unit (as shown in Scheme 1). Each layer of the dendrimer is conventionally named as 'Generation *N*', where *N* represents how far the each layer is apart from the core; for example, Generation 1



**Scheme 1.** Molecular structure of the third generation poly(propylene imine) dendrimer with a 1,4-diaminobutane (DAB) core: ellipsoids for denoting the generation number that the each polymer repeat unit belongs to.

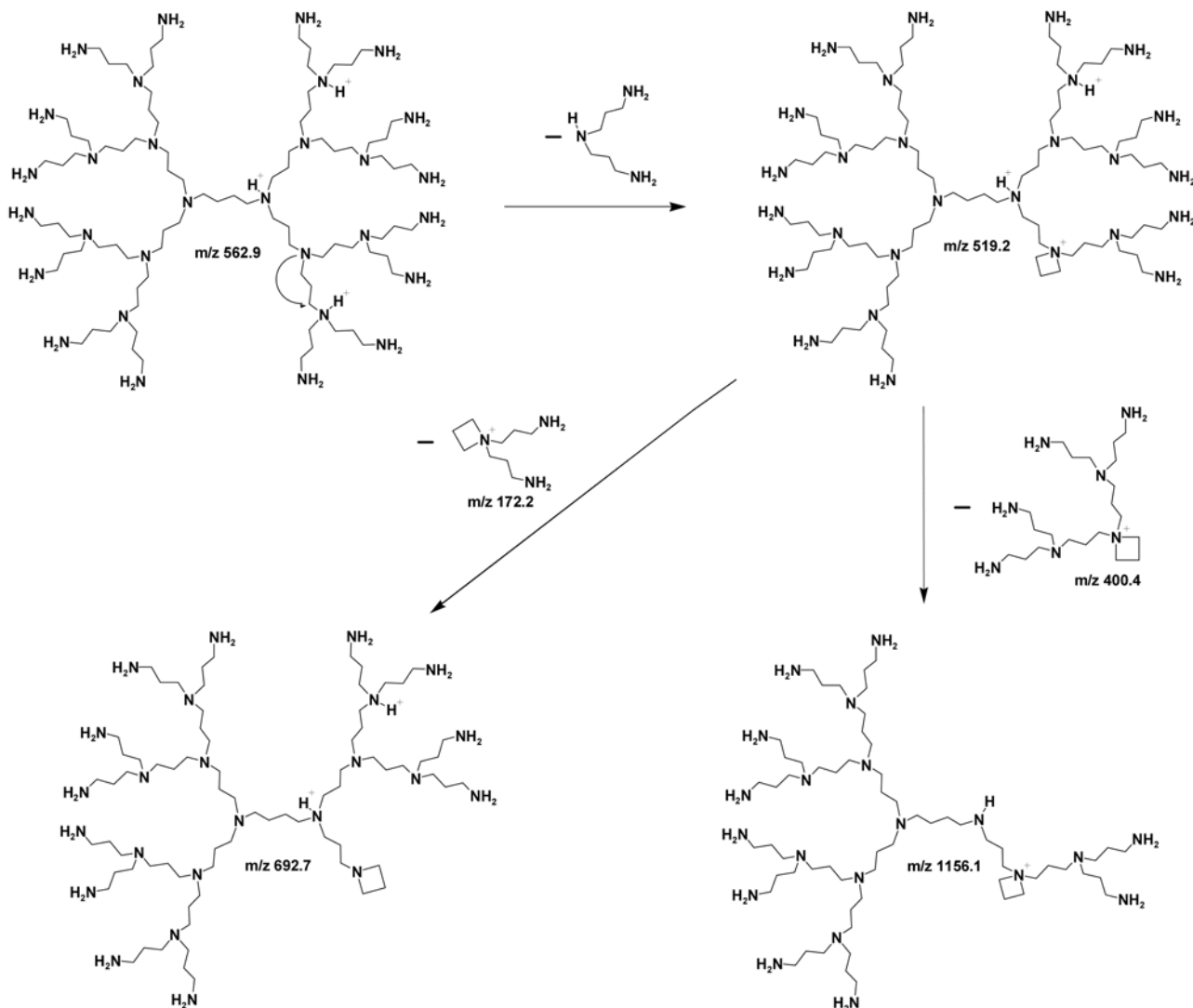
<sup>a</sup>Both authors contribute equally to this article.

denotes the first layer away from the core. The largest generation number of a given dendrimer is also used for referring the size of the dendrimer; the dendrimer in Scheme 1 is referred to as the 3<sup>rd</sup> generation dendrimer.

The complex structure of this polymer was previously confirmed by MALDI-TOF, SID (surface induced dissociation), and ESI ion-trap tandem mass spectrometry (MS/MS).<sup>7-9</sup> In particular, McLuckey and his coworkers investigated the dissociation behaviors of the generation 1-5 upon collisional activation, in detail, under ion-trap conditions.<sup>9</sup> Thereby, it was demonstrated that fragmentation is generally driven by the nucleophilic attack of a nearest-neighbor nitrogen onto the carbon alpha to a protonation site (tertiary amine) (see Scheme 2). This finding enables one to directly correlate the fragmentation sites with the protonated locations, thus proton distribution among various generations within this dendritic polymer. Particular attention needs to be paid to this finding as the current experimental studies are designed and performed based upon this

observation. The charge (proton) driven fragmentation was also shown to be dependent upon the precursor-ion charge state; singly-charged ions fragment preferably in the lower generations (layers), whereas the ions of higher charge states do so in the higher generations. Frequent fragmentations in certain generations can be understood in terms of minimization of Coulombic repulsion that is induced by multiple numbers of protons of positive charge. That is, in the high charge states, scattering of multiple protons could be most effectively achieved by distributing the protons in the higher generations.

Expectedly, structures of dendritic polymers can also be analyzed using a relatively new tandem mass spectrometry method of electron capture dissociation (ECD MS). Indeed, a series of hyperbranched polyesteramides polymers were successfully studied using ECD MS by Heeren and his coworkers.<sup>10</sup> However, ECD MS is actually now more widely used for peptide/protein structural analyses.<sup>11-13</sup> In ECD, an electron that is passing by a positively-charged



**Scheme 2.** Fragmentation pathway leading to the detected signals at  $m/z$  172.2, 400.4, 519.2, 692.7, and 1156.1, respectively. As a result of the nucleophilic attack of a nitrogen onto the alpha carbon to a protonated tertiary amine, two amine product ions are generated; one is a quaternary amine ion and the other is a primary amine.

molecular ion is captured by protons in the molecular ion, thus yielding a neutralized hydrogen atom,  $H^\bullet$ . The neutralized  $H^\bullet$ -atom can follow two possible subsequent reaction pathways; one is toward the backbone dissociation of the polymer ions as in the peptide/proteins ECD, the other is toward the ejection of the resultant  $H^\bullet$ -atom out of the main molecule (as will be utilized for the current MS studies). Among many aforementioned ECD events, the focus of the present study is on the process of electron capture by a proton since electron capture is the starting point of the ECD procedure and also relatively fewer considerations, either experimental or theoretical, have so far been provided with for the understanding of this process.

In contrast to the proton distribution as revealed by collisional activation dissociation (CAD) fragmentation patterns, the electron capture efficiencies of the protons show another interesting structural aspect of the dendrimer ions. Upon electron irradiation under ECD experimental conditions, a multiple number of protons within the complex dendritic structure will compete for the incoming electron. Their efficiencies in electron capture are expected to vary depending on their locations in the dendrimer with a complex branched architecture. A general expectation is that the protons located in the inner layers (generations) would have lower electron capture efficiency than the ones in the outer generations, due to all the possible capture sites that an incoming electron may pass by during its approach toward the core of the dendrimer. However, a contradictory statement that an electron, as a quantum mechanical element, may not be sensitive at all to such capture sites ubiquitous during its approach sounds plausible as well. Thus, a rigorous experimental verification is necessary before any conclusion is established.

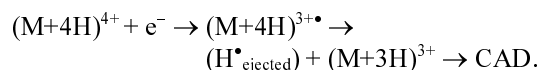
In the present report, the 3<sup>rd</sup> generation dendrimer of  $M_r = \sim 1.7$  kDa is under investigation as this size of a polymer provides a good analogy to the peptide ions that are frequently met in the mass spectral analysis of peptide mixtures. Thus, the information obtained in the current investigation may carry an interesting implication for the case of peptide ECD MS. The description of the experiment and its results will be given below in detail.

### Experimental Section

Experiments were performed on a commercial 4.7 Tesla Fourier transform mass spectrometer (FTMS: Ionspec, Lake Forest, CA, USA) equipped with a modified nano-electrospray source. Detailed description of the experimental setup can also be found elsewhere.<sup>14,15</sup> In brief, 50  $\mu$ M poly(propylene) imine DAB dendrimer (3<sup>rd</sup> generation, monoisotopic mass = 1685.7 : Aldrich, Seoul) was prepared in 49 : 49 : 2  $CH_3OH : H_2O : CH_3COOH$  solution, and was directly infused through a fused silica capillary spray tip (I.D. = 100  $\mu$ m) at a flow rate of 1-10  $\mu$ L/min using a syringe pump (Havard apparatus 22, Holliston, MA, USA). Sprayed ions were accumulated for 0.25-0.5 sec in a hexapole trap before

being transferred through a single stage rf-only ion-guide into the ICR (ion cyclotron resonance) cell. Each charge state of trapped precursor ions was isolated using a SWIFT (Stored Waveform Inverse Fourier Transform) waveform tailored for the respective  $m/z$  windows of interest.<sup>16</sup>

In order to gain the information we are aiming for, applications of a combination of two tandem mass spectrometry methods, ECD + SORI-CAD, are necessary. At a first sight, it appears that ECD MS is sufficient by itself for revealing the electron capture efficiencies for the protons in the different layers of the dendrimer, but it is not (see below). Thus, in the present study, a new experimental strategy combining both tandem mass spectrometry techniques is devised for the first time. Its detailed experimental procedure is as follows. First, multiple protons in the native 4+ ions (occurring from electrospray ionization) are allowed to compete for an electron under normal ECD conditions. As a result, the proton with the higher electron capture efficiency will react more readily with the incoming electron to yield a  $H^\bullet$ -atom, which will be consequently ejected out of the dendrimer as shown in an earlier literature from our group. The remaining molecular ion obtained after  $H^\bullet$ -atom ejection then corresponds to the 3+ ion whose charge is reduced to 3+, thus so-called reduced 3+ ion. Application of CAD on the reduced 3+ ion will provide the information regarding the distribution of the protons that are left after the electron capture. Hence, the electron capture efficiency of the protons in the different layers of the 4+ dendrimer can be learned indirectly from the data obtained above. The whole sequence of this new experimental strategy can be schematically summarized in the following:



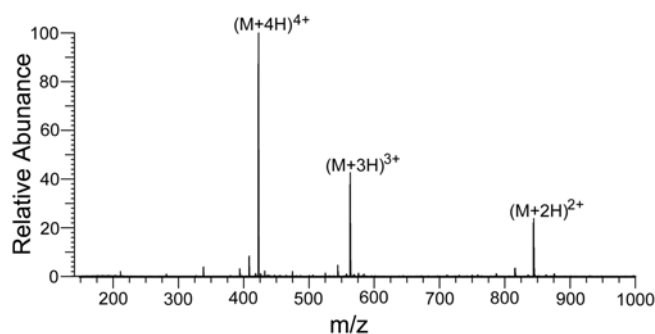
Electron capture experiments were performed following the conventional ECD procedures.<sup>11-13</sup> Electron beam was generated on the surface of the heated dispenser cathode (Heatwave Labs, Watsonville, CA, USA) located just outside the ICR cell. The electron kinetic energy and the beam current were found to be most important experimental parameters. The former was controlled in the range of 0.35-0.45 eV and the latter was optimized at 5 V potential applied to the cathode. Collisional activation dissociation was achieved by utilizing +1.0 kHz sustained off-resonance irradiation (SORI-CAD).<sup>17</sup> Dissociation power was controlled by adjusting SORI-CAD application amplitude in Volt so that  $\sim 20\%$  of precursor ions survived SORI-CAD. All the MS/MS spectra were averaged over 20 scans. Each experiment was repeated for at least three times in order to get meaningful statistics. The resulting MS/MS spectra were zero-filled once and then subjected to one Hanning apodization procedure, and subsequently analyzed manually without any aid of retrieving/interpreting software due to the unconventional character of the sample molecules. The sample was used as provided from a commercial vendor, without further purification.

## Results and Discussion

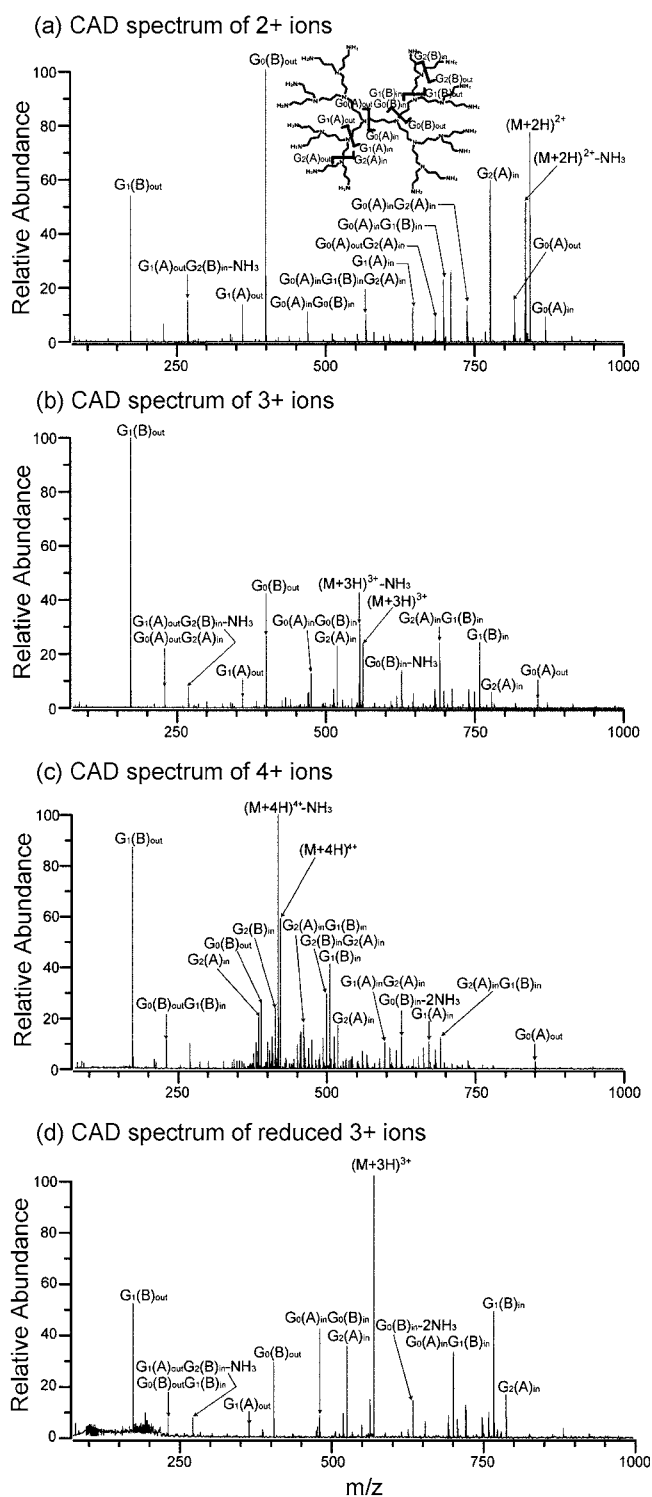
### Electrospray Mass Spectrum of Native Dendrimer Ions.

Figure 1 displays the mass spectra obtained by electro-spraying 50  $\mu\text{M}$  poly(propylene) imine DAB dendrimer (Generation 3,  $M_r = 1685.7$  Da) prepared in 49 : 49 : 2  $\text{CH}_3\text{OH} : \text{H}_2\text{O} : \text{CH}_3\text{COOH}$  solution. As shown in Figure 1, this spectrum contains multiple abundant peaks at  $m/z$  422.7 ( $(M+4\text{H})^{4+}$ ), 563.3 ( $(M+3\text{H})^{3+}$ ), and 844.4 ( $(M+2\text{H})^{2+}$ ) as well as numerous signals of low abundance. The highly abundant signals observed at  $m/z$  422.7, 563.3, and 844.4 represent the multiply protonated molecules of the dendrimer, each of which carries 4+, 3+, and 2+ ions, respectively, whereas the low abundant peaks are synthetic failures or the ions fragmented presumably in the nozzle-skimmer region. Changes in the composition of ESI solution resulted in variation of the relative abundances for the precursor ions, but did not produce 1+ or 5+ ions that were abundant enough to allow for further tandem mass spectrometry analysis. Thus, in the following experiments, only 2+ 4+ ions,  $(M+n\text{H})^{n+}$  [ $n = 2-4$ ], are chosen for further characterization of the proton distribution and electron capture efficiencies of the protons.

**SORI-CAD on 2+ – 4+ Precursor Dendrimer Ions.** MS/MS fragmentation behaviors of multiply protonated molecules were investigated by means of SORI-CAD tandem mass spectrometry. First, doubly-charged precursor ions,  $(M+2\text{H})^{2+}$ , were isolated and then subjected to SORI-CAD, resulting in the MS/MS spectrum of Figure 2(a). In total, 42 fragment ions are produced, which much surpasses  $\sim 10$  ions previously observed in the ion-trap experiment by McLuckey *et al.*<sup>9</sup> The increased number of fragmented ions is due largely to the enhanced sensitivity of the employed mass spectrometry analyzer, *i.e.* Fourier-transform ion cyclotron resonance mass spectrometer. In contrast to the ion-trap results, our spectrum includes a large number of fragments that are generated with double covalent bond cleavages, responsible for  $\sim 30\%$  of all the products. In addition, the fragmentation behaviors for 3+ and 4+ ions were also probed, yielding 67 and 63 fragment ions, respectively. The results obtained here for the 3+ and 4+ ions were not previously measured using different types of mass spectrometry analyzers such as the ion-trap, MALDI-TOF, and SID



**Figure 1.** Electrospray mass spectrum for the native precursor ions of the dendrimer.



**Figure 2.** SORI-CAD MS/MS spectra for (a) 2+ precursor ions,  $(M+2\text{H})^{2+}$ , (b) 3+ precursor ions, (c) 4+ precursor ions, and (d) the reduced 3+ ions. The cleavage sites are also denoted in the inset of (a): the molecular skeleton of poly(propylene imine) dendrimer. Notations for the detected  $m/z$  signals are as follows. The generation number,  $G_x$ , denotes the generation each protonated nitrogen, under a nucleophilic attack, belongs to; for example, the nitrogens in a 1,4 diaminobutane core are assignable to  $G_0$  and the nitrogens in the very next generation are to  $G_1$ , and so on. A or B in the parenthesis denotes whether the interior nitrogen attacks on the alpha carbon in the exterior or vice versa, respectively.

MS.<sup>7-9</sup>

Assignment of the fragment ions is achieved by following the nomenclature and cleavage scheme suggested previously.<sup>7-9</sup> As an illustrating example, a fragmentation pathway leading to the signals at  $m/z$  172.2, 400.4, 519.2, 692.7, and 1156.1 is depicted in Scheme 2, which also reflects the nucleophilic attack of a basic nitrogen onto the alpha carbon to a protonated amine. Assigned fragments are all categorized based upon the generation in which the dissociation occurs, with its result represented in Figure 3 (see also Figure Caption 2 for the details of the notations). Here it is to be noted that the categorization in Figure 3 is made for 'Generation 0-2' only, not including 'Generation 3', though the dendrimer under the current investigation is the third generation one. It is because the proton affinity of a primary amine (terminal amine) is significantly smaller than that of a tertiary amine (*e.g.*, 912.0 vs. 981.8 kJ/mol, for the primary amine and the tertiary ethylamine, respectively) and more importantly, its resultant fragmentation leading to an  $\text{NH}_3$  loss can be caused by different mechanisms other than the nucleophilic attack described above.<sup>18</sup>

In accordance with previous literatures, the 2+ ions with low charge density dissociate frequently closer to the core, that is, in 'Generation 0' ( $G_0$ ). As the charge state increases, the weight of fragmentation preference is observed to shift a little toward the higher generations. This trend is well illustrated in Figure 3(e), where the fractional fragmentation in  $G_0$  (FF0) decreases as the charge state of the precursor ions increases; this value is observed to monotonously decrease from 40% (2+ ions) to 20% (4+ ions) with a certain reproducibility. In contrast, FF1 and FF2 do not appear to reflect the characteristics of the dendrimer charge states as clearly as FF0 does. For example, in the case of FF1, the values for 3+ and 4+ ions are similar in the range of 42-45%, while that for 2+ ions is less than 30%. Nevertheless, when characterizing an unknown fragmentation spectrum, all the FF values for Generation 0-2 are, however, expected to be very useful, in a collective manner, in relating it with the characteristics of the known charge state (see below).

As suggested in previous literatures, fragmentation sites can be correlated directly with the protonation sites. As a matter of fact, assignments for the fragment ions are here all made on the assumption of this correlation.<sup>9</sup> Thus it suggests that the analysis in Figure 3 should represent the proton distributions for the each charge state, which is consistent with the relieved Coulomb repulsion in the higher charge states by locating the protons farther away, *i.e.*, in the higher generations.

### 3+ Ions Reduced from Electron Capture by 4+ Ions.

For the investigation of the electron capture efficiencies of the protons belonging to the three different generations in the 4+ dendrimer ion,  $G_x$  ( $x = 0, 1, \text{ or } 2$ ), a new strategy is devised, which involves the comparison between the native 2+ - 4+ ions and the reduced 3+ ions (from electron capture) in their SORI-CAD fragmentation behaviors, *i.e.*, their proton distribution among the three generations. This strategy utilizes the fact that the 3+ ions derived from

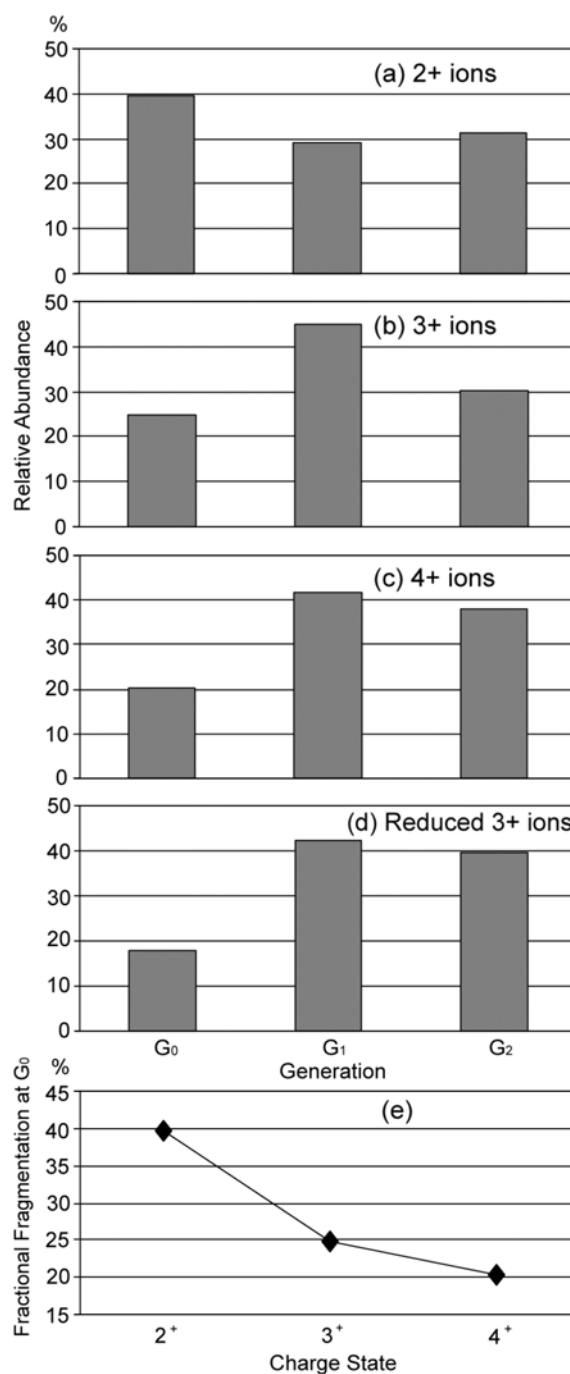


**Figure 3.** Analysis of SORI-CAD fragment ions based upon the generation to which the protonated nitrogen, under the nucleophilic attack, belongs, for (a) 2+ ions, (b) 3+ ions, (c) 4+ ions, and (d) the reduced 3+ ions. (e) Fractional fragmentation at  $G_0$  (FF0) denoted as a function of the precursor ions.

charge-reduction (*i.e.*, electron capture) of 4+ ions lack in the specific proton having higher electron affinity.<sup>19</sup>

In order to facilitate the designed experiment, *i.e.*, SORI-CAD on the reduced 3+ ions, the abundance of the reduced 3+ ions was maximized by adjusting the experimental parameters such as an electron beam time, electron current, and electron kinetic energy.<sup>11</sup> As shown in the earlier literature from our group, ECD for the 4+ dendrimer ions,

$(M+4H)^{4+}$ , resulted mostly in the 3+ molecular ions with one hydrogen atom ejected,  $(M+3H)^{3+}$ , which was confirmed by high-accuracy mass measurement.<sup>15</sup> This result is well described in Figure 4, where ECD of the isolated 4+ ions (a) mainly gives the reduced 3+ ions (b). The abundance of the reduced 3+ ions amounts to as much as ~30% of the 4+ ions. In a separate experiment for the native 3+ ions, the abundance of the reduced 2+ ions was too low for the subsequent SORI-CAD analysis of the reduced 2+ ions.

In the 4+ ions, the proton with higher electron affinity readily combines with an electron to produce an energetic hydrogen atom,  $H^\bullet$ , with ~6 eV exothermicity, followed by  $H^\bullet$  ejection from an intermediate radical cation species of  $(M+4H)^{3+}$ ;  $(M+4H)^{4+} + e^- \rightarrow [(M+4H)^{3+}]_{hot} \rightarrow (M+3H)^{3+} + (H^\bullet)_{ejected}$ .<sup>19</sup> This intermediate species are also often observed in the ECD experiments for peptide/protein ions, but contrastingly as a minor channel.<sup>11-13,19</sup> In peptide/protein ions, the presence of a peptide bond in the vicinity of an incipient  $H^\bullet$  radical site provides reaction pathways leading mainly to the bond cleavage between an amide nitrogen and the alpha carbon ( $C_\alpha$ ), so-called *c*, *z* $^\bullet$  cleavage, or to the bond dissociation of  $C(O)-NH$  (see Equation 1 and 2 below). The lack of this kind of functional groups in the dendrimer manifold appears to be responsible for the dominant  $H^\bullet$  ejection, *i.e.*, the reduced 3+ ions.<sup>15,19</sup>

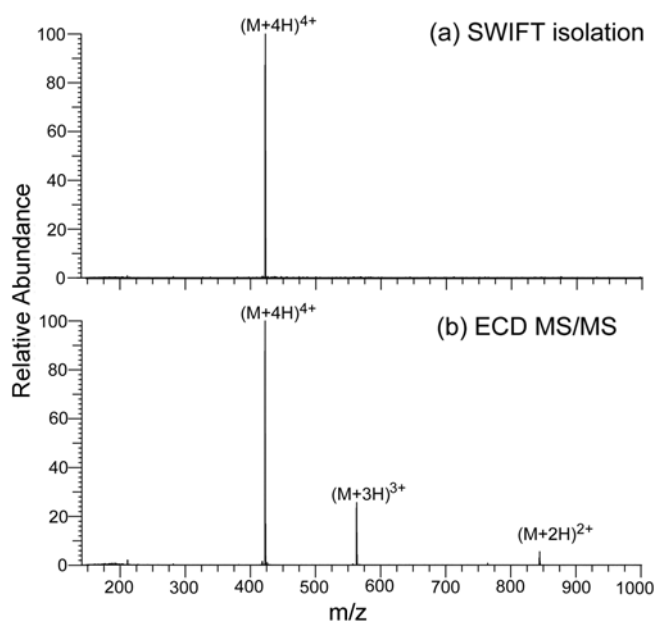
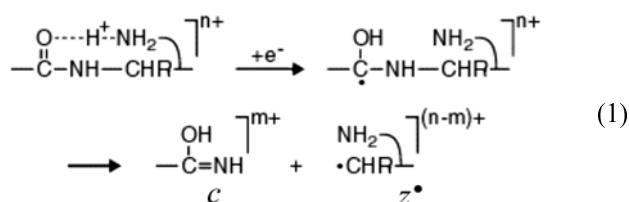
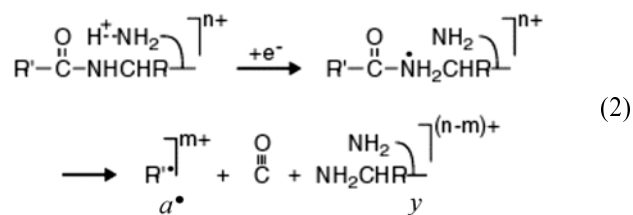


**Figure 4.** (a) Mass spectrum showing the isolation of the native 4+ ions by a SWIFT waveform and (b) MS/MS spectrum obtained as a result of ECD application for the 4+ ions: the singly-reduced 3+ ions at *m/z* 563 and doubly-reduced 2+ ions at *m/z* 844.



**SORI-CAD on the Reduced 3+ Ions.** SORI-CAD for the reduced 3+ ions was performed successfully to give 25 fragment ions, which represents a much smaller number of fragments compared to the SORI-CAD spectrum for the native 3+ ions (25 vs. 67 product ions). Analysis of the spectrum is also achieved based upon the generation of the fragmentation sites (see Figure 5a). Interestingly, the analysis results for the reduced 3+ ions are found almost identical to those for the native 4+ ions within an experimental uncertainty (also see Figure 3). The reduced 3+ ions underwent fragmentations with the FF values for  $G_{0,2}$  being 18, 42, and 40%, respectively, which is very close to 20, 42, and 38% for the native 4+ ions. However, the obtained FF values show a distinguishable discrepancy against those for the native 3+ ions with 25, 45, and 30% relative abundances. Particularly, the FF0 value of 18%, which is demonstrated above as the clearest indicator for determining the characteristics associated with the charge state of an unknown fragmentation spectrum, suggests a close similarity in the obtained charge characteristics to that for the native 4+ ions.

A close resemblance of both SORI-CAD fragmentation behaviors indicates very similar proton distributions in the both 3+ reduced ions and native 4+ ions since the fragmentation behaviors can be directly linked with the

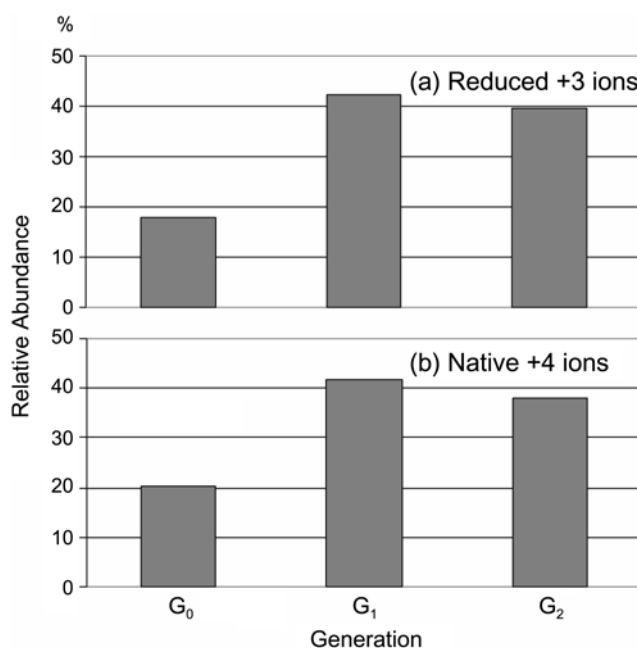


**Figure 5.** Analysis of the fragment ions from SORI-CAD of (a) the reduced 3+ ions, and (b) the naturally-occurring 4+ ions shown again for clear comparison with (a).

proton distribution among the different generations of the dendrimer. In other words, the analysis made above can be understood in terms of the retained proton distribution in the reduced 3+ ions even after electron capture by the protons on the native 4+ ions. This retained proton distribution is possible only when the protons belonging to the different generations of the dendrimer have comparable electron capture efficiencies, despite the variation in the molecular environments by which the each generation is encompassed. Different capture efficiencies would, if any, result in a change in the proton distribution of the reduced 3+ ions, from that of the native 4+ ions.

This observation is somewhat contradictory to the common expectations that the protons in the inner generations may not be well exposed to the incoming electron as much as the outer ones are, thus may be less efficient for electron capture. For this size of a dendrimer ( $M_r \sim 1.7$  kDa, Generation 3), it seems that the capture probability in the outer generations that the incoming electron may experience during its penetration into the core,  $G_0$ , is not high enough to cause incomparable efficiencies. Larger dendrimer ions may have the structures congested enough to bring about prominently different capture efficiencies, and thus its investigation is now under way.

On the other hand, this unbiased electron capture efficiencies within the dendrimer polymer ion offer a hint toward the understanding of ECD MS results for small peptide ions. For the peptide ions, ECD MS has been, in general, found to give no obvious site-specific fragmentations.<sup>20</sup> Since the peptide ions of 1-2 kDa mass are expected to have much less structural complexity, comparable electron capture efficiencies within the hyperbranched polymer ions of  $\sim 1.7$  kDa strongly suggests that the protons in the small peptide ions have more or less equivalent electron capture efficiencies, regardless of their locations.

In summary, CAD fragmentation behaviors for the 2+ – 4+ precursor ions of the third generation poly(propylene imine) dendrimers are studied using the SORI-CAD tandem mass spectrometry. It reveals that each charge state assumes a varying proton distribution among the three different generations, *i.e.*, in  $G_{0-2}$ . Based upon this, the proton distribution in the reduced 3+ ions is investigated using a newly devised methodology employing both SORI-CAD and ECD methods, exhibiting almost identical proton distribution to that for the native 4+ ions. This observation suggests that the protons in the polymer ions with a size of  $\sim 1.7$  kDa be more

or less equivalent in terms of electron capture efficiency.

**Acknowledgments.** The authors are grateful to Prof. Gyusung Chung and Prof. Duckhwan Lee for helpful discussions. SL and HBO are thankful to Sunghyun Yu, Jaedong Kim, and Iljoon Lee for their helps in experiments and discussions. This work was supported by Korea Research Foundation Grant (R08-2003-000-10493-0).

## References

1. Boas, U.; Heegaard, P. M. H. *Chem. Soc. Rev.* **2004**, 33, 43.
2. Scott, R. W. J.; Wilson, O. M.; Oh, S.-K.; Kenik, E. A.; Crooks, R. M. *J. Am. Chem. Soc.* **2004**, 126, 15583.
3. Suk, J.; Lee, J.; Kwak, J. *Bull. Korean Chem. Soc.* **2004**, 25, 1681.
4. Neubert, H.; Knights, K. A.; de Miguel, Y. R.; Cowan, D. A. *Macromolecules* **2003**, 36, 8297.
5. Fenn, J. B.; Mann, M.; Meng, C. K.; Wong, S. F.; Whitehouse, C. M. *Science* **1989**, 246, 64.
6. Tanaka, K.; Waki, H.; Ido, Y.; Akita, S.; Yoshida, Y.; Yoshida, T. *Rapid Commun. Mass Spectrom.* **1988**, 2, 151.
7. Tang, X.-J.; Thibault, P.; Boyd, R. K. *Anal. Chem.* **1993**, 65, 2824.
8. Jones, J. L.; Dongre, A. R.; Somogyi, A.; Wysocki, V. H. *J. Am. Chem. Soc.* **1996**, 116, 8368.
9. McLuckey, S. A.; Asano, K. G.; Schaaff, G.; Stephenson J. L. Jr. *Int. J. Mass Spectrom.* **2000**, 195/196, 419.
10. Koster, S.; Duursma, M. C.; Boon, J. J.; Heeren, M. A.; Ingemann, S.; van Benthem, R. A. T. M.; de Koster, C. G. *J. Am. Soc. Mass Spectrom.* **2003**, 14, 332.
11. Zubarev, R. A.; Horn, D. M.; Fridriksson, E. K.; Kelleher, N. L.; Kruger, N. A.; Lewis, M. A.; Carpenter, B. K.; McLafferty, F. W. *Anal. Chem.* **2000**, 72, 563.
12. Oh, H. B.; Brueker, K.; Sze, S. K.; Ge, Y.; Carpenter, B. K.; McLafferty, F. W. *Proc. Natl. Acad. Sci. USA* **2002**, 99, 15863.
13. Breuker, K.; Oh, H. B.; Lin, C.; Carpenter, B. K.; McLafferty, F. W. *Proc. Natl. Acad. Sci. USA* **2004**, 101, 13971.
14. Yu, S.; Lee, S.; Chung, G.; Oh, H. B. *Bull. Korean Chem. Soc.* **2004**, 25, 1477.
15. Lee, S.; Han, S. Y.; Lee, T. G.; Lee, D.; Chung, G.; Oh, H. B. submitted to *J. Am. Soc. Mass Spectrom.* (2005).
16. Marshall, A. G.; Wang, T. C. L.; Ricca, T. L. *J. Am. Chem. Soc.* **1985**, 107, 7893.
17. Gauthier, J. W.; Trautman, T. R.; Jacobson, D. B. *Anal. Chim. Acta* **1991**, 246, 211.
18. NIST Chemistry Webbook: <http://webbook.nist.gov/chemistry/>.
19. Breuker, K.; Oh, H. B.; Cerda, B. A.; Horn, D. M.; McLafferty, F. W. *Eur. J. Mass Spectrom.* **2002**, 8, 277.
20. Hakansson, K.; Chalmers, M. J.; Quinn, J. P.; McFarland, M. A.; Hendrickson, C. L.; Marshall, A. G. *Anal. Chem.* **2003**, 75, 3256.